Electronic Supplementary Information For

Rapid Self-Healing and Anion Selectivity in Metallosupramolecular Gels Assisted by Fluorine-Fluorine Interactions

Leticia Arnedo-Sánchez,[a] Nonappa,[b] Sandip Bhowmik,[a] Sami Hietala,[c] Rakesh Puttreddy,[a] Manu Lahtinen[a], Luisa De Cola[d] and Kari Rissanen[a*]

[a.] *Nanoscience Center, Department of Chemistry, University of Jyväskylä, P.O. Box. 35, Jyväskylä, FI-40014, Finland. E-mail. Kari.t.rissanen@jyu.fi*
[b.] *Molecular Materials Group, Department of Applied Physics, Aalto University School of Science, FI-02150, Espoo.*
[c.] *Laboratory of Polymer Chemistry, Department of Chemistry, University of Helsinki, P.O. Box 55, FI-00014, Helsinki.*
[d.] *ISIS, Université de Strasbourg and CNRS UMR 7006, 8 rue Gaspard Monge, Strasbourg 67000, France*

Table of Contents

Synthesis and characterization

All the reactions were carried out under inert atmosphere (Schlenk technique) and all the solvents were used as received from Sigma without any further purification. 4′-chloro-2,2′:6′,2″-terpyridine, 4-aminophenylboronic acid pinacol ester, pentadecafluorooctanoyl chloride and pentadecafluorooctanoyl chloride were purchased from Sigma and used as received. The compounds were purified by column chromatography using neutral alumina 0.063-0.200 mm (70 - 230 mesh ASTM) as stationary phase. ^{1}H, ^{13}C and ^{19}F NMR spectra were recorded on a Bruker Avance III HD 300 and DRX 400 NMR spectrometer. The ^{1}H NMR chemical shifts (δ) are given in ppm and referred to residual protons on the corresponding deuterated solvent. All deuterated solvents were used as received without any further purification. All coupling constants (J) are given in Hertz (Hz). Mass spectra were recorded on a micromass (ESI-TOF) spectrometer.

4-Aminophenyl-2,2´:6´,2´´-terpyridine (2)

4´-Chloro-2,2´:6´,2´´-terpyridine (500.0 mg, 1.87 mmol), 4-aminophenylboronic acid pinacol ester (499.2 mg, 2.28 mmol, 1.2 equiv.), sodium carbonate (593.8 mg, 5.60 mmol, 3eq) and $[Pd(PPh_3)_4]$ (151.1 mg, 0.13 mmol, 0.07 eq) were placed in a Schlenk flask, degassed and placed under argon. This process was repeated for three times. Previously degassed dimethoxyethane (30 mL) was added to the Schlenk flask and the reaction mixture was degassed. Previously degassed deionized water (7.5 mL) was added and the reaction mixture degassed. The solution was heated up to 90 ^{o}C for 72 h. After cooling down to room temperature, the reaction mixture was diluted with dichloromethane, washed with saturated NH_4Cl, brine, dried ($MgSO_4$) and evaporated to get the crude product. The crude product was purified by recrystallization from boiling ethanol solution. Yield 90%. ^{1}H NMR (300 MHz, $CDCl_3$, 25 °C) δ/ppm: 8.74–8.75 (m, 2H), 8.72 (s, 2H), 8.67-8.67 (d, 2H, J 8.0 Hz), 7.99 (td, 2H, J 1.7, 7.7 Hz), 7.78-7.80 (d, 2H, J 2.0, 8.5 Hz), 7.37 (td, 2H), 6.79-6.81 (d, 2H, J 2.1 8.4Hz). ^{13}C NMR (100 MHz, $CDCl_3$, 25 °C) δ/ppm: 156.6, 155.9, 150.0, 149.2, 147.7, 137.0, 128.7, 128.4, 123.8, 121.5, 118.0, 115.4. HRMS (ESI-TOF) m/z calcd. for $[M+H]^+$ $(C21H17N4)^+$: 325,1448; found: 325.1423.

N-(4-([2,2':6',2''-Terpyridin]-4'-yl)phenyl)-2,2,3,3,4,4,5,5,6,6,7,7,8,8,8-pentadecafluorooctanamide (3)

4-Aminophenyl-2,2´:6´,2´´-terpyridine (500mg, 1.54mmol) was dissolved in dry DCM (50 mL). N,N-Diisopropylethylamine (806 µL, 4.63 mmol) was added to the stirred solution and the resulting mixture was stirred at RT for 30 minutes. The reaction mixture was cooled down to 0 ^{o}C and pentadecafluorooctanoyl chloride (574 µL, 2.31 mmol) was added dropwise. The reaction mixture was let to warm up to RT and stirred overnight. After 16 h, the solvent was evaporated and the remaining brown solid was purified by column chromatography (neutral alumina, hexane: ethyl acetate 4:1) to give gave 854 mg white powder (77% yield). ^{1}H NMR (300 MHz, 298 K, CDCl$_3$) δ/ppm: 8.75 (m, 4H), 8.69 (d, J = 8.0 Hz, 2H), 8.01 (s,1H), 7.98 (d, J = 8.6 Hz 2H), 7.91 (td, J = 7.8, 1.7 Hz, 2H), 7.74 (d, J = 8.7 Hz, 2H), 7.38(td, J = 6.0, 0.7 Hz, 2H),.^{13}C NMR (75 MHz, 298 K, DMSO-d_6), δ/ppm:155.59, 154.87, 148.88, 148.31, 136.89, 134.61, 127.16, 123.94, 121.81, 120.60, 117.45, 110.01, ^{19}F NMR (470 MHz, CDCl$_3$): -83.74(s), -122.07(s), -124.32(s), -124.83(s), -125.06(s), -125.59(s), -129.01(s). HRMS (ESI-TOF) m/z calcd. for [M+H]$^+$ (C29H16F15N4O)$^+$: 721.1079; found: 721.1078. Single crystals suitable for X-ray analysis were obtained upon slow evaporation of chloroform solution.

N-(4-([2,2':6',2''-Terpyridin]-4'-yl)phenyl)octanamide (3H)

4-Aminophenyl-2,2´:6´,2´´-terpyridine (50mg, 0.15 mmol) was taken in a dry Schelnk tube and the reaction vessel was degassed by purging argon several times. Dry DCM (5 mL) and *N,N*-diisopropylethylamine (80 µL, 0.46 mmol, 3 eq.) was added and the resulting mixture was stirred at RT for 30 minutes. The reaction mixture was cooled down to 0 ^{o}C and octanoyl chloride (50 µL, 0.31 mmol, 2 eq.) was added dropwise. The reaction mixture was allowed to warm up to RT and stirred for 16 h. The crude product obtained after solvent evaporation was purified by column chromatography (neutral alumina, hexane: ethyl acetate 4:1 as eluent). ^{1}H NMR (300 MHz, CDCl$_3$, 25 °C) δ/ppm: 8.73 (d, J = 3.8 Hz, 2H), 8.71 (s, 2H), 8.66 (d, J = 7.5 Hz 2H), 7.86-7.90 (m, 4H), 7.68 (d, J = 8.1 Hz,2H), 7.35 (t, J = 6.0 Hz, 2H), 7.31(s, 1H) 2.38 (t, J = 7.3 Hz, 2H), 1.75 (m, 2H), 1.30 (m, 8H), 0.89 (t, J = 6.8 Hz, 3H) ^{13}C NMR (75 MHz, 298 K, CDCl$_3$) δ 156.43, 156.03, 149.28, 149.23, 137.05, 128.13, 123.99, 121.54, 119.95, 118.57, 38.08, 31.82, 29.39, 29.19, 25.69, 22.77, 14.23. HRMS (ESI-TOF) m/z calcd. for [M+H]$^+$ (C29H31N4O)$^+$: 451.2492; found: 451.2528.

N-(4-([2,2':6',2''-Terpyridin]-4'-yl)phenyl)-4,4,5,5,6,6,7,7,8,8,9,9,10,10,11,11,11-heptadecafluoroundecanamide (4)

4-Aminophenyl-2,2´:6´,2´´-terpyridine (500 mg, 1.54 mmol) was placed in a Schlenk flask, degassed and placed under argon. This process was repeated for three times. Dry DCM (50 mL) and *N,N*-diisopropylethylamine (806 µL, 4.63 mmol, 3 eq) was added to the stirred solution and the resulting mixture was stirred at RT for 30 minutes. The reaction mixture was cooled to 0 ^{o}C and 4,4,5,5,6,6,7,7,8,8,9,9,10,10,11,11,11-heptadecafluoroundecanoyl chloride (1575.83 mg, 3.09 mmol, 2 eq) was added. The reaction mixture was allowed to warm up to RT and stirred overnight. After 16 h, the solvent was evaporated to obtain the crude product. The crude product was purified by column chromatography (neutral alumina, hexane: ethyl acetate 4:1 as eluent).Yield 43%.^{1}H NMR (400 MHz, 298 K, $CDCl_3$) δ/ppm: 8.74 (d, J = 5.2 Hz, 2H), 8.72 (s, 2H), 8.67 (d, J = 8.0 Hz, 2H), 7.86-7.92 (m, 4H), 7.67 (d, J = 8.3 Hz, 2H), 7.36 (td, J = 6.6, 1.1 Hz 2H), 7.33(s, 1H), 2.60-2.74 (m,4H) ^{13}C NMR (101MHz, 298 K, $CDCl_3$), δ/ppm:,168.15, 156.35, 156.08, 149.49, 149.25, 138.49, 137.09, 134.62, 128.20, 124.04, 121.58, 120.18, 118.62, 28.26, 26.50 ^{19}F NMR (470 MHz, 298 K, $CDCl_3$) δ -83.72, -115.44, -122.23, -122.46, -123.22, -123.89, -126.42. HRMS (ESI-TOF) m/z calcd for $[M+H^{+}]^{+}$ (C32H20F17N4O)$^{+}$: 799.1360; found: 799.1355.

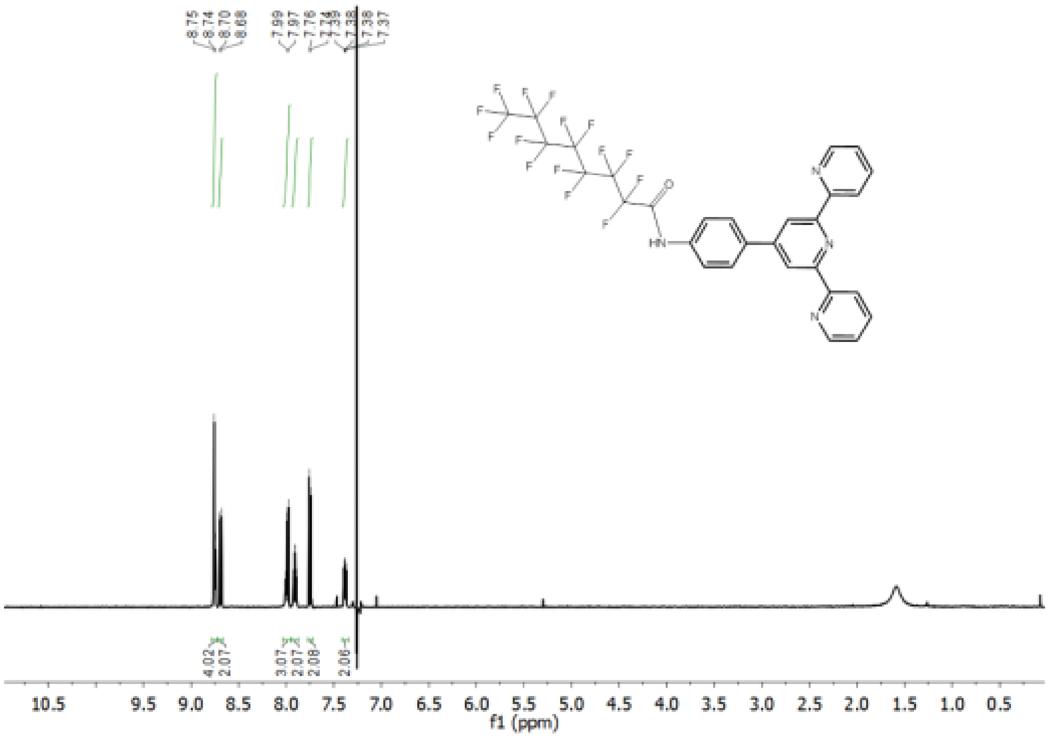

Figure S1. ^{1}H NMR (300 MHz, 298 K) spectrum of ligand **3** in $CDCl_3$.

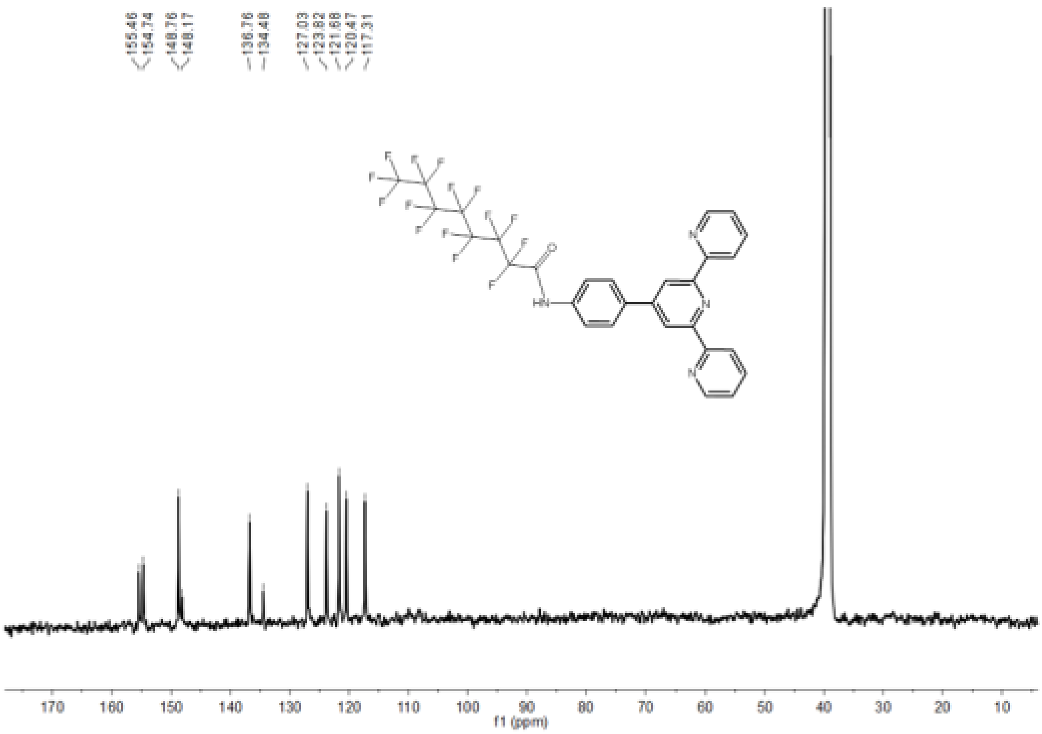

Figure S2. ^{13}C NMR (75 MHz, 298 K) spectrum of ligand **3** in DMSO-d_6.

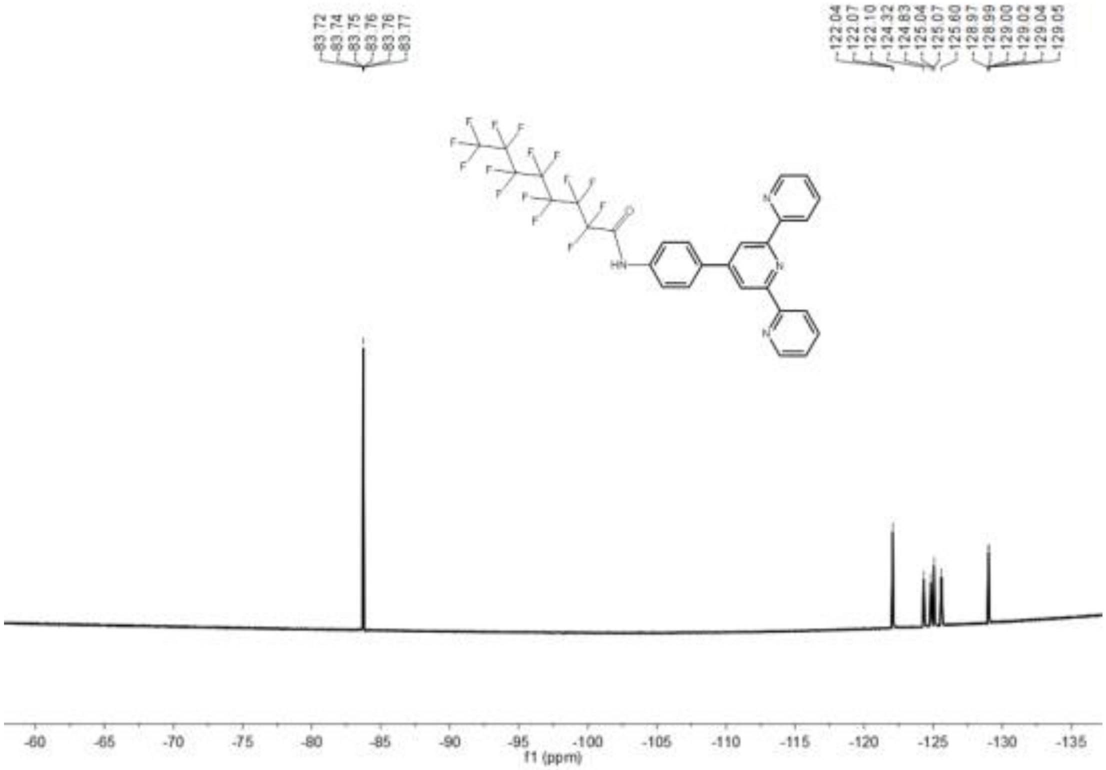

Figure S3. ^{19}F NMR (470 MHz, 298 K) spectrum of ligand **3** in $CDCl_3$.

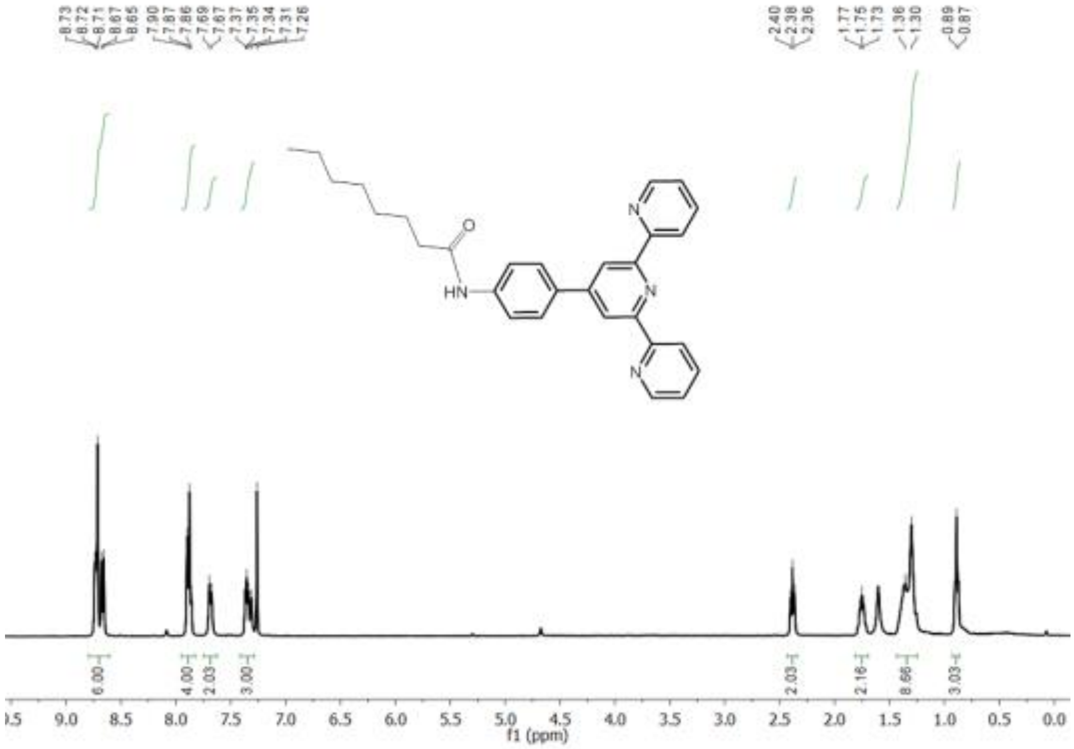

Figure S4. ^{1}H NMR (300 MHz, 298 K)spectrum of ligand **3H** in $CDCl_3$.

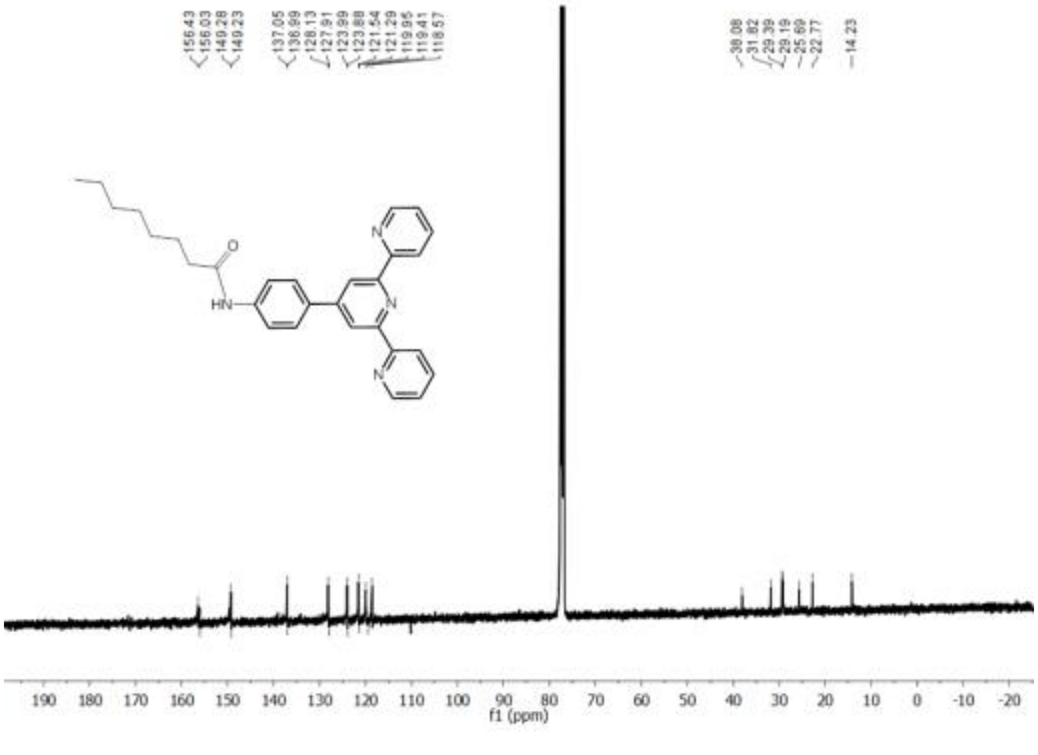

Figure S5. ^{13}C NMR (75 MHz, 298 K)spectrum of ligand **3H** in $CDCl_3$.

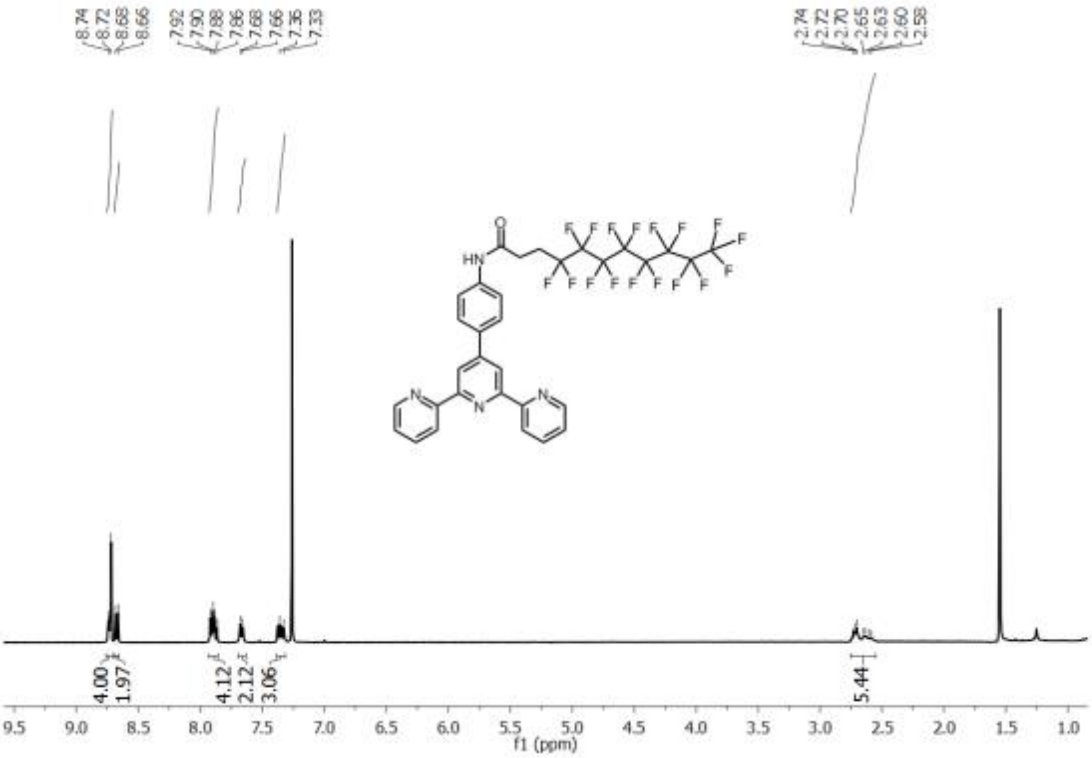

Figure S6. ^{1}H NMR (400 MHz, 298 K)spectrum of ligand **4** in $CDCl_3$

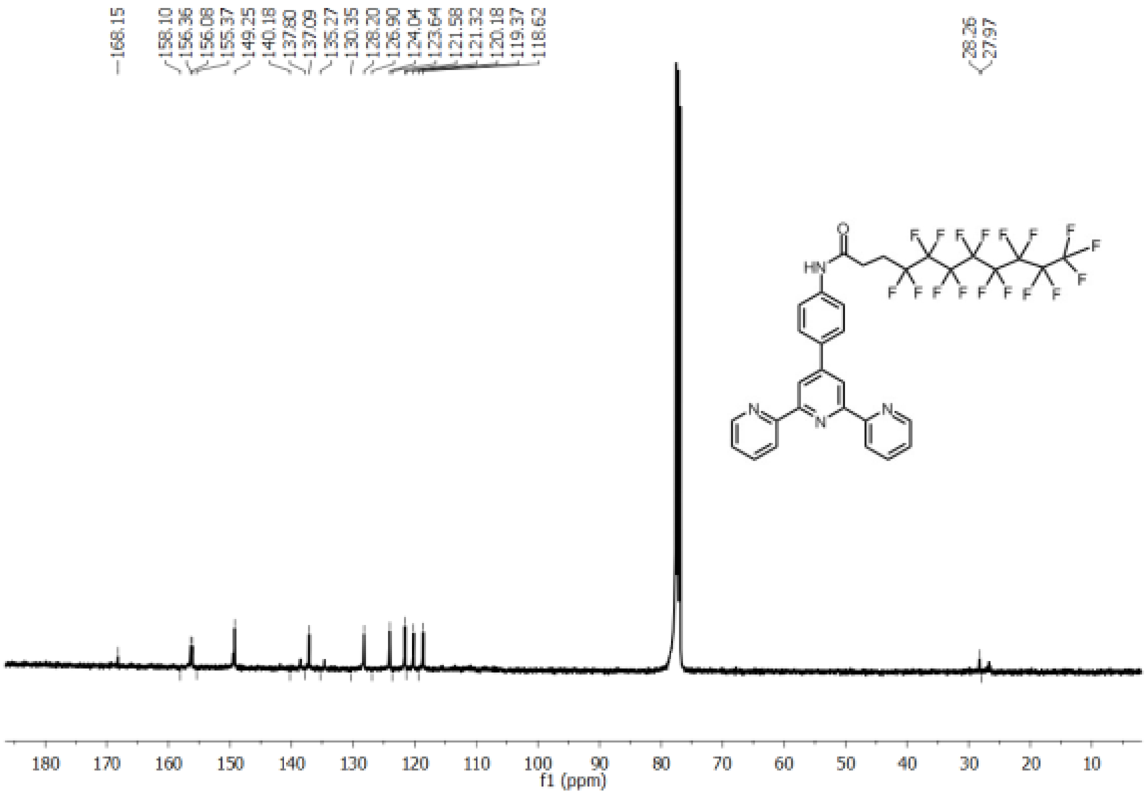

Figure S7. ^{13}C NMR (101 MHz, 298 K)spectrum of ligand **4** in $CDCl_3$.

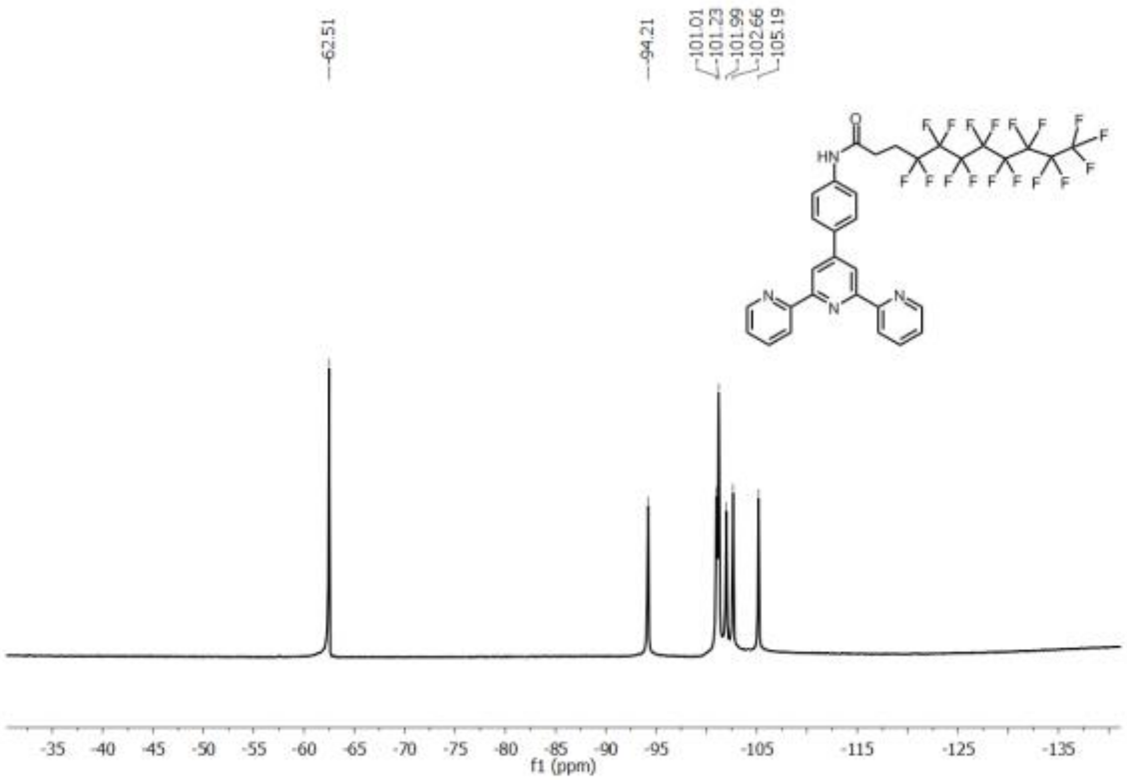

Figure S8. ^{19}F NMR (470 MHz, 298 K)spectrum of ligand **4** in $CDCl_{3.}$

Scanning electron microscopy (SEM)

The sample preparation for SEM was performed by preparing a 2 w/v% metallogel. The gel was then heated until it turned into a clear solution and drop casted over a carbon tape placed over aluminium stub. The sample was then allowed to dry under ambient conditions subjected from sputter coating with Au under vacuum conditions at 20 mA for 1 min. The samples were then subjected for imaging with Sigma Zeiss scanning electron microscope.

Transmission electron microscopy (TEM)

The transmission electron microscopy (TEM) images were collected using FEI Tecnai G2 operated at 120 kV and JEM 3200FSC field emission microscope (JEOL) operated at 300 kV in bright field mode with Omega-type Zero-loss energy filter. The images were acquired with GATAN DIGITAL MICROGRAPH software while the specimen temperature was maintained at -187 ^{o}C. The TEM samples were prepared by drop casting 3-5 µL of the hot solution of a pre-made gel on to a 400 mesh copper grid with holey carbon support film. The samples were dried under ambient condition prior to imaging.

Rheological measurements

TA AR2000 stress controlled rheometer equipped with 20 mm steel plate and a Peltier heated plate was used for rheological characterization. The measuring setup was covered with a sealing lid in order to prevent evaporation during the measurements. Measurements were performed using oscillation frequency of 6.284 rad/s unless otherwise noted. Temperature ramps from 20 to 90°C were made with 5 °C/min heating rate, while all the other experiments were made at 20°C. For the step strain experiments controlled strain of 0.1% and 150% were used, respectively.

Gelation studies

In a typical gelation test, 4.0 mg of ligand **3** was dissolved in 172 µL DMSO in a test tube ($d \approx 1.0$ cm) by heating. To the ligand solution, 28 µL of MX_2 (M=Fe(II), Ni(II), Co(II); X= Cl^-, Br^-, BF_4^-, ClO_4^-, SO_4^{2-} or OTf^-) 0.1 M aqueous solution was added. The resulted mixture was heated to get a homogeneous solution. The sample was then allowed to attain room temperature. The sample was considered a gel if it did not flow upon inversion.

Minimum gelation concentration (MGC)

Gels of different concentrations were prepared as mentioned above. The lowest concentration at which the sample was stable against gravity upon inversion was taken as the *mgc*.

Anion selectivity

Gelation tests were carried out by mixing 4 mg of free gelator **3** suspended in 172 µL DMSO with 28 µL of the corresponding FeX_2 (X= Cl^-, Br^-, BF_4^-, ClO_4^-, SO_4^{2-} or OTf^-) (0.1M, aq). The aggregates turned immediately into purple upon addition of the metal. The mixture was melted by heating and allowed to attain room temperature. In all cases except Cl^-, a thick purple solution was obtained instead of a gel. Then 2.8 µL aqueous NaCl (1.0 M) solution was added to the vial and the sample was melted again by heating. Upon cooling down a gel was obtained.

Mass spectrometry of metallogels

3-Fe: MS (ESI-TOF) m/z calcd for $[M]^{+2}$ $(C_{58}H_{30}F_{30}FeN_8O_2)^{2+}$: 748.07; found: 748.71.

3-Co: MS (ESI-TOF) m/z calcd for $[M]^{+2}$ $(C_{58}H_{30}F_{30}CoN_8O_2)^{+2}$: 749.57; found: 749.57.

3-Ni: MS (ESI-TOF) m/z calcd for $[M]^{+2}$ $(C_{58}H_{30}F_{30}CoN_8O_2)^{+2}$: 749.07; found: 749.07.

PXRD

The X–ray powder diffraction data were made with PANalytical X´Pert PRO diffractometer in Bragg–Brentano geometry using Cu Kα radiation (1.5418 Å with 45kV, 40mA power settings). Powder-like samples were prepared on a silicon-made zero–background holder using petrolatum jelly as an adhesive. The data was recorded from a spinning sample by X´Celerator detector using continuous scanning mode in 2θ range of 4–60° with a step size of 0.017° and counting times of 100 or 150 s per step. Diffraction data analyses were carried out with PANalytical HighScore Plus v. 4.5 program. Simulated X-ray diffraction pattern was produced with program Mercury v. 3.8 using crystallographic parameters of the corresponding single crystal structure.

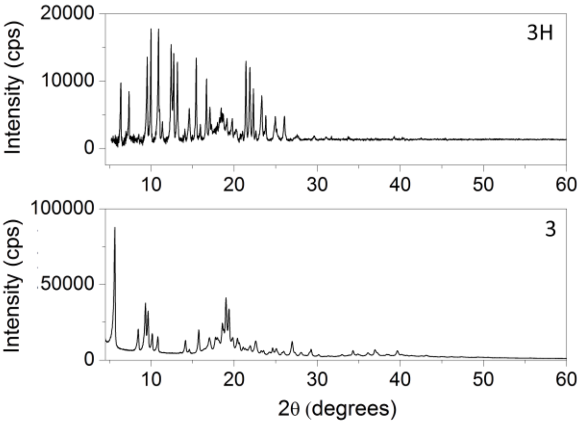

Figure S9. Comparison of PXRD pattern of dry aggregates of ligand **3H** (top) and **3** (bottom).

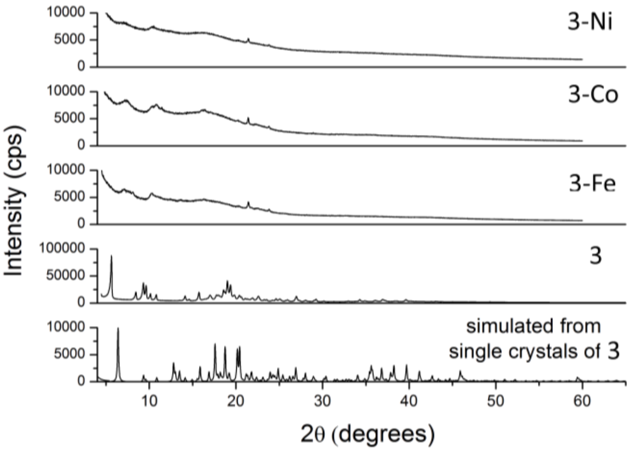

Figure S10. PXRD patterns of xerogels of **3, 3-Fe, 3-Co** and **3-Ni** and simulated PXRD pattern from single crystals of **3**.

T_{gel} studies

Sealed gel samples were placed upside-down in a thermostated oil bath. The temperature of the bath was raised at a rate of 1°C/min. The temperature at which the gel starts to flow was taken as the T_{gel} of the sample.

Table S1. T_{gel} data for gels **3-Fe** and **3-Co**.

	T_{gel}-Mean value (^{o}C)	
v/w%	**3-Fe gel**	**3-Co gel**
1.2	56.5	38.3
1.4	58.3	40.7
1.6	60.7	42.5
1.8	63.6	45.4
2.0	69.7	47.1
2.2	73.2	49.8
2.4	79.9	52.9

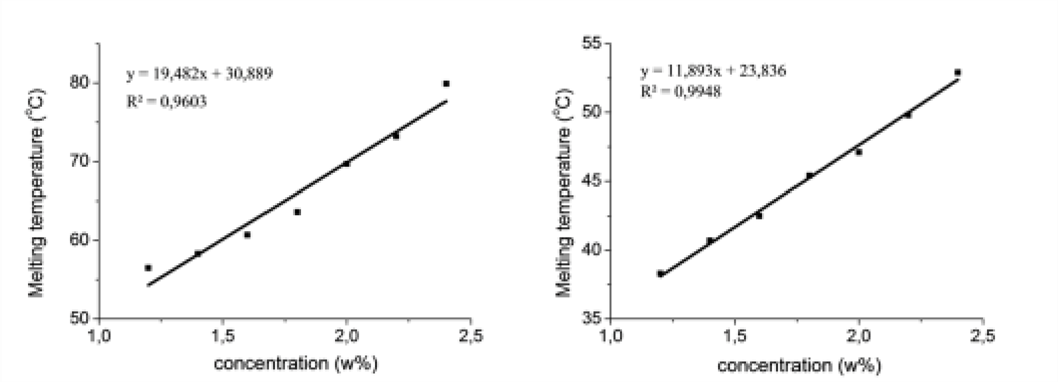

Figure S11. T_{gel} vs concentration for gels **3-Fe** (left), and **3-Co** (right).

Single crystal X-ray diffraction

Single crystal X-ray data for **3, 3·CHCl$_3$, 3·THF, 3·CH$_3$OH·H$_2$O** and **[Ni4$_2$]Cl$_2$** were collected either at 120 K or 123 K on dual source Rigaku SuperNova diffractometer equipped with an Atlas detector using multilayer optics monochromated Cu-Kα (λ = 1.54184 Å) radiation. The data collection, reduction and gaussian face index absorption correction were performed using *CrysAlisPro*[1] All structures were solved with direct methods (*SHELXS)*,[2] and refined by full-matrix least squares on F^2 using the *OLEX2* program package,[3] which utilizes the *SHELXL*-2014 refinement module.[4] Constraints and restraints are used where appropriate for the disordered perfluoroalkyl chains. For all the structures, no attempt was made to locate the hydrogen atoms from Fourier difference map, and all H-atoms were included in the refinement in the calculated positions on the riding atoms using ADDH command in *OLEX2*.

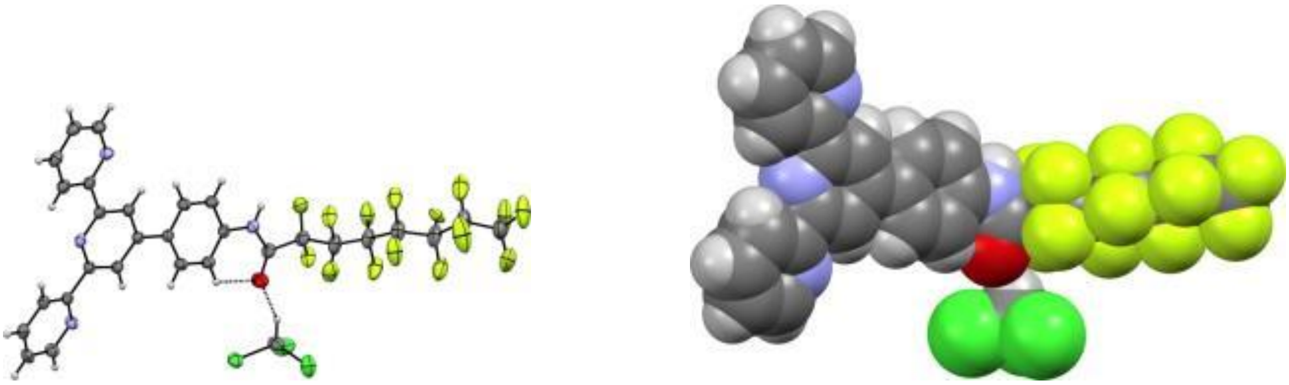

Figure S12. Crystal structure of ligand **3·CHCl$_3$** with thermal displacement parameters at 50% probability level (left) and a CPK model (right). The perfluorinatedalkyl chain is disordered and the other orientation is removed for clarity. Hydrogen bonding is shown with a dotted line.

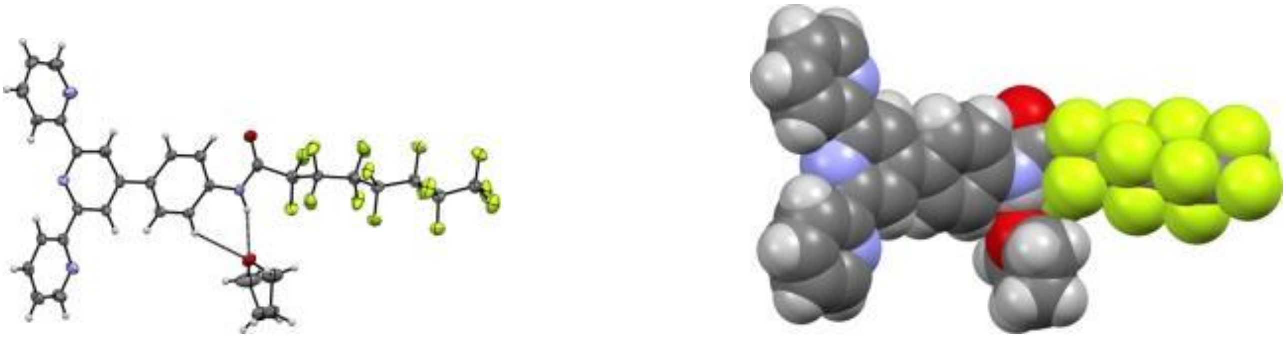

Figure S13. Crystal structure of the ligand **3·THF** with thermal displacement parameters at 50% probability level (left) and a CPK model (right). The perfluorinated alkyl chain is not disordered. Hydrogen bonding is shown with dotted lines.

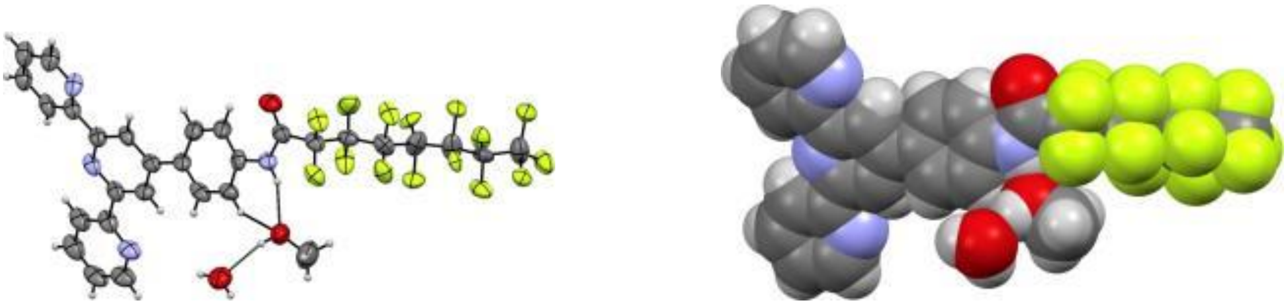

Figure S14. Crystal structure of ligand **$3 \cdot CH_3OH \cdot H_2O$** with thermal displacement parameters at 50% probability level (left) and a CPK model (right). The perfluorinatedalkyl chain is disordered and the other orientation is removed for clarity. Hydrogen bonding is shown with dotted lines.

Figure S15. Picture of **4-Ni** gel showing crystals of **$[Ni4_2]Cl_2$** growing inside the gel matrix.

Table S2. Crystallographic data for compounds **3, 3.CHCl$_3$** and **3.THF.**

Identification code	**3**	**3·CHCl$_3$**	**3·THF**
CCDC No.	1533110	1533113	1533112
Empirical formula	$C_{29}H_{15}F_{15}N_4O$	$C_{30}H_{16}Cl_3F_{15}N_4O$	$C_{33}H_{24}F_{15}N_4O_2$
Formula weight	720.45	839.82	793.56
Temperature/K	120.0(1)	123.0(3)	123.0(1)
Crystal system	orthorhombic	monoclinic	orthorhombic
Space group	$Pca2_1$	$P2_1/n$	$P2_1cn$
a/Å	9.7840(2)	5.62249(13)	5.7081(5)
b/Å	10.0744(2)	60.950(3)	10.0000(7)
c/Å	55.262(1)	9.3539(3)	56.029(4)
α/°	90	90	90
β/°	90	99.250(3)	90
γ/°	90	90	90
Volume/Å^3	5447.1(2)	3163.84(19)	3198.2(4)
Z	8	4	4
ρ_{calc}g/cm^3	1.757	1.763	1.648
μ/mm^{-1}	1.628	3.779	1.470
F(000)	2880.0	1672.0	1600.0
Crystal size/mm^3	0.209 × 0.143 × 0.024	0.0833 × 0.0409 × 0.039	0.179 × 0.038 × 0.022
Radiation	CuKα (λ = 1.54184)	CuKα (λ = 1.54184)	CuKα (λ = 1.54184)
2Θ range for data collection/°	8.778 to 133.492	8.704 to 133.492	8.982 to 133.456
Index ranges	$11 \leq h \leq 11$, $-12 \leq k \leq 12$, $-65 \leq l \leq 65$	$-4 \leq h \leq 6$, $-72 \leq k \leq 48$, $-11 \leq l \leq 8$	$-6 \leq h \leq 6$, $-11 \leq k \leq 11$, $-66 \leq l \leq 66$
Reflections collected	82852	9579	44193
Independent reflections	9628 [R_{int} = 0.0404, R_{sigma} = 0.0203]	5545 [R_{int} = 0.0320, R_{sigma} = 0.0454]	5656 [R_{int} = 0.1024, R_{sigma} = 0.0613]
Data/restraints/parameters	9628/1/883	5545/27/643	5656/1/487
Goodness-of-fit on F^2	1.057	1.041	1.066
Final R indexes [I>=2σ (I)]	R_1 = 0.0349, wR_2 = 0.0929	R_1 = 0.0489, wR_2 = 0.1163	R_1 = 0.0726, wR_2 = 0.1411
Final R indexes [all data]	R_1 = 0.0377, wR_2 = 0.0954	R_1 = 0.0636, wR_2 = 0.1262	R_1 = 0.0833, wR_2 = 0.1468
Largest diff. peak/hole / e Å^{-3}	0.30/-0.23	0.32/-0.35	0.56/-0.34

Table S3. Crystallographic data for compounds **$3.CH_3OH.H_2O$** and **$[Ni4_2]Cl_2$**.

Identification code	**$3{\cdot}CH_3OH{\cdot}H_2O$**	**$[Ni4_2]Cl_2$**
CCDC No.	1533114	1533111
Empirical formula	$C_{30}H_{21}F_{15}N_4O_3$	$C_{68}H_{52}Cl_2F_{34}N_8NiO_5S_2$
Formula weight	770.51	1900.90
Temperature/K	120.0(1)	120.0(1)
Crystal system	monoclinic	triclinic
Space group	*Pn*	*P*-1
a/Å	5.5175(6)	10.4507(7)
b/Å	31.498(3)	13.2384(8)
c/Å	9.0538(9)	26.961(2)
α/°	90	95.396(6)
β/°	99.36(1)	91.534(6)
γ/°	90	90.814(5)
Volume/Å^3	1552.5(3)	3711.7(4)
Z	2	2
ρ_{calc}g/cm^3	1.648	1.701
μ/mm^{-1}	1.518	2.865
F(000)	776.0	1912.0
Crystal size/mm^3	0.073 × 0.032 × 0.024	0.127 × 0.082 × 0.034
Radiation	CuKα (λ = 1.54184)	CuKα (λ = 1.54184)
2Θ range for data collection/°	8.422 to 133.466	6.708 to 133.492
Index ranges	$-6 \le h \le 6$, $-37 \le k \le 37$, $-10 \le l \le 10$	$-12 \le h \le 9$, $-15 \le k \le 15$, $-32 \le l \le 32$
Reflections collected	22314	20793
Independent reflections	5503 [R_{int} = 0.0892, R_{sigma} = 0.0721]	13059 [R_{int} = 0.0547, R_{sigma} = 0.1108]
Data/restraints/parameters	5503/8/585	13059/12/1318
Goodness-of-fit on F^2	1.052	1.027
Final R indexes [I>=2σ (I)]	R_1 = 0.0618, wR_2 = 0.1401	R_1 = 0.0792, wR_2 = 0.1987
Final R indexes [all data]	R_1 = 0.1008, wR_2 = 0.1652	R_1 = 0.1278, wR_2 = 0.2329
Largest diff. peak/hole / e Å^{-3}	0.28/-0.21	0.94/-1.37

NMR Spectroscopy studies

All samples were left to equilibrate for 5 min upon reaching the desired temperature. A DMSO-*d*$_6$ solution of fluorobenzene (2M) was employed as external standard to monitor the signal intensity. The external standard was previously calibrated by using a DMSO-*d*$_6$ solution of o-bromofluorobenzene (0.5M).

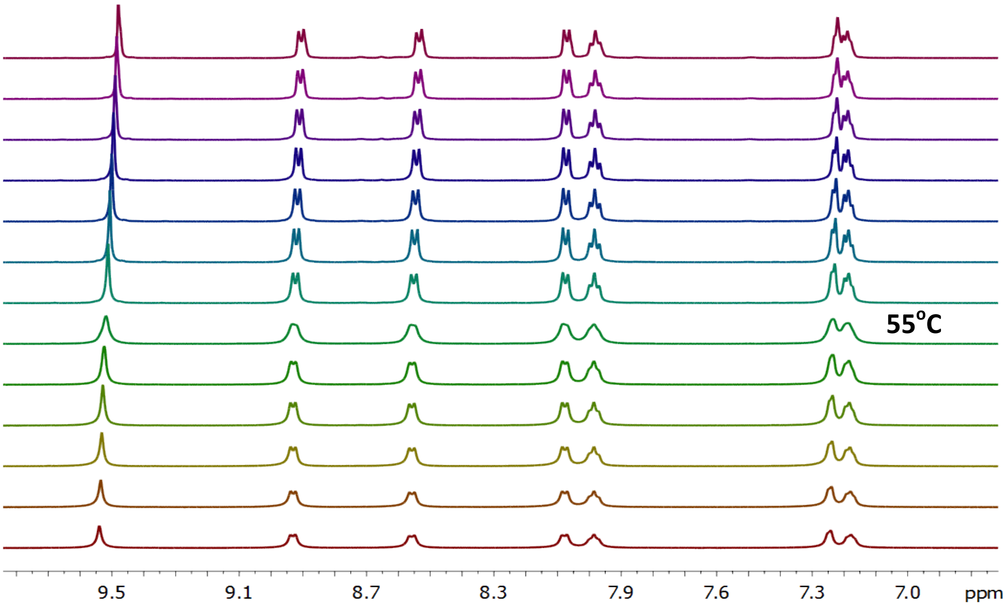

Figure S16. Partial VT ^{1}H NMR (400 MHz) spectra of **3-Fe** gel 2% DMSO-d6-D$_2$O. The spectra were collected from 30 °C (bottom) to 90 °C (top) with 5 °C increments.

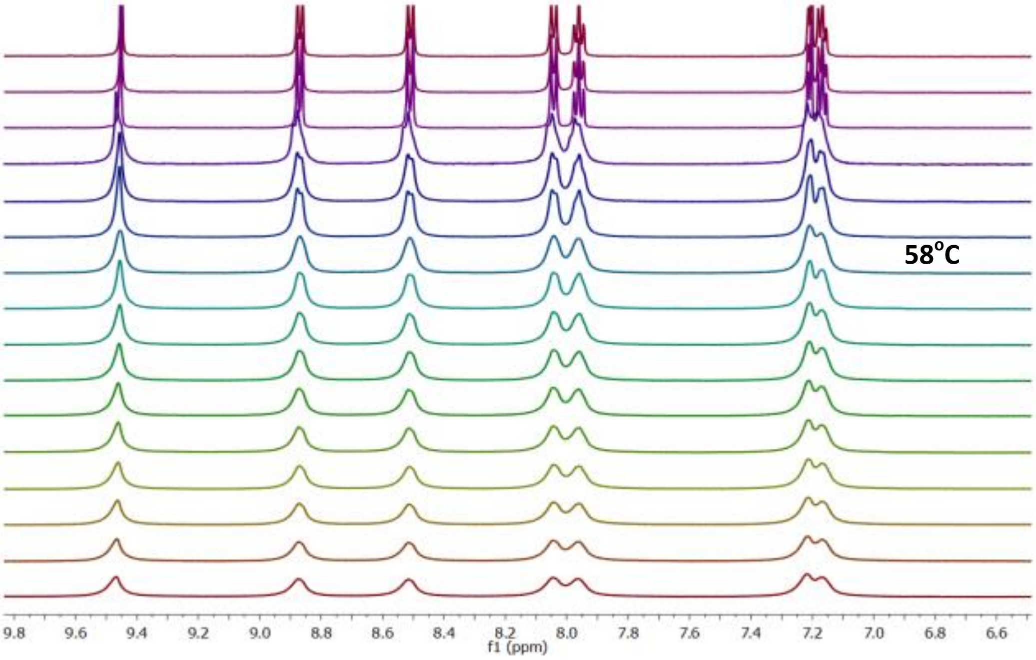

Figure S17. Partial VT ^{1}H NMR (400 MHz) spectra of **3-Fe** gel 2% DMSO-d$_6$-D$_2$O. The spectra were collected from 40 °C (bottom) to 70 °C (top) with 2 °C increments.

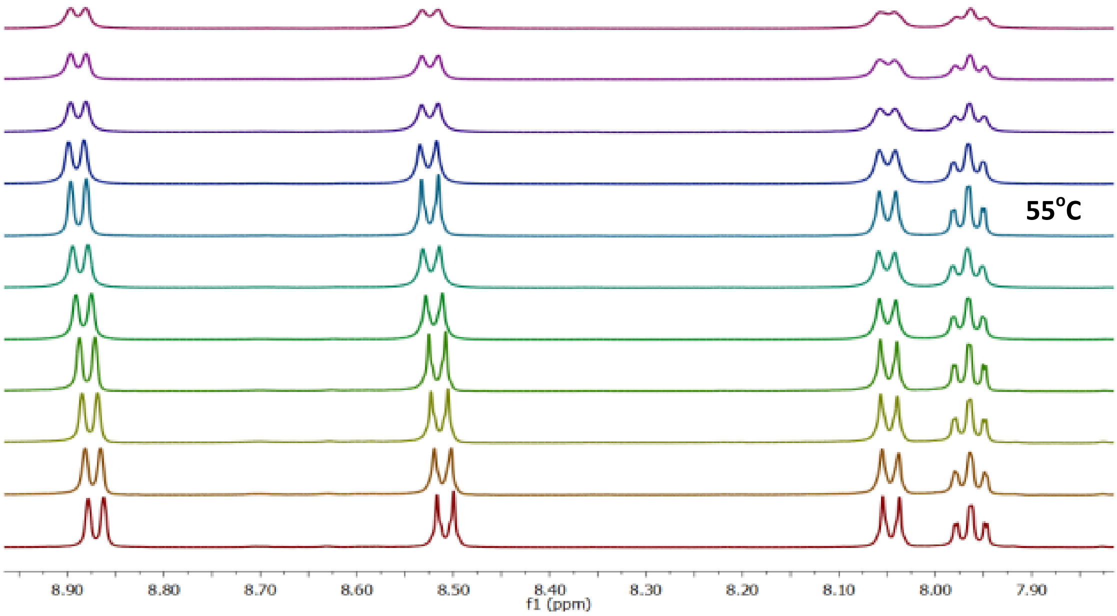

Figure S18. Partial VT ^{1}H NMR (400 MHz) spectra of **3-Fe** gel 2% DMSO-d_6-D_2O. The spectra were collected from 85 °C (bottom) to 35 °C (top) with 5 °C decrements.

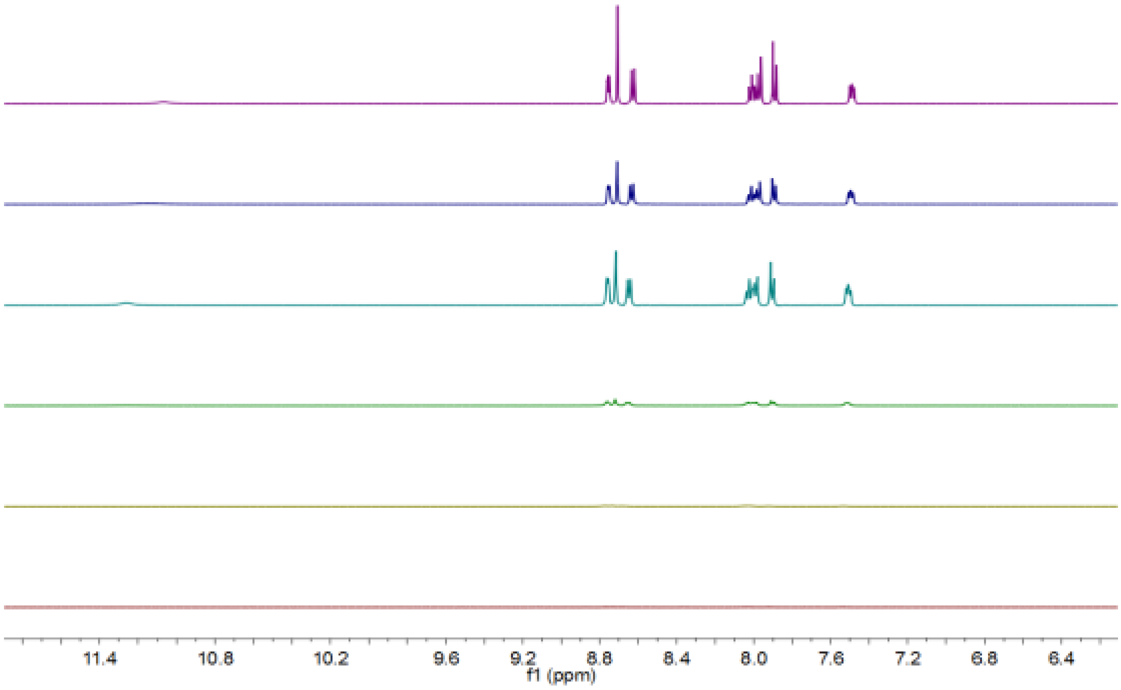

Figure S19. VT ^{1}H NMR (400 MHz) free ligand **3**, 2% DMSO-d_6-D_2O. The spectra were collected from 25 °C (bottom) to 120 °C (top) with 15 or 20 °C increments.

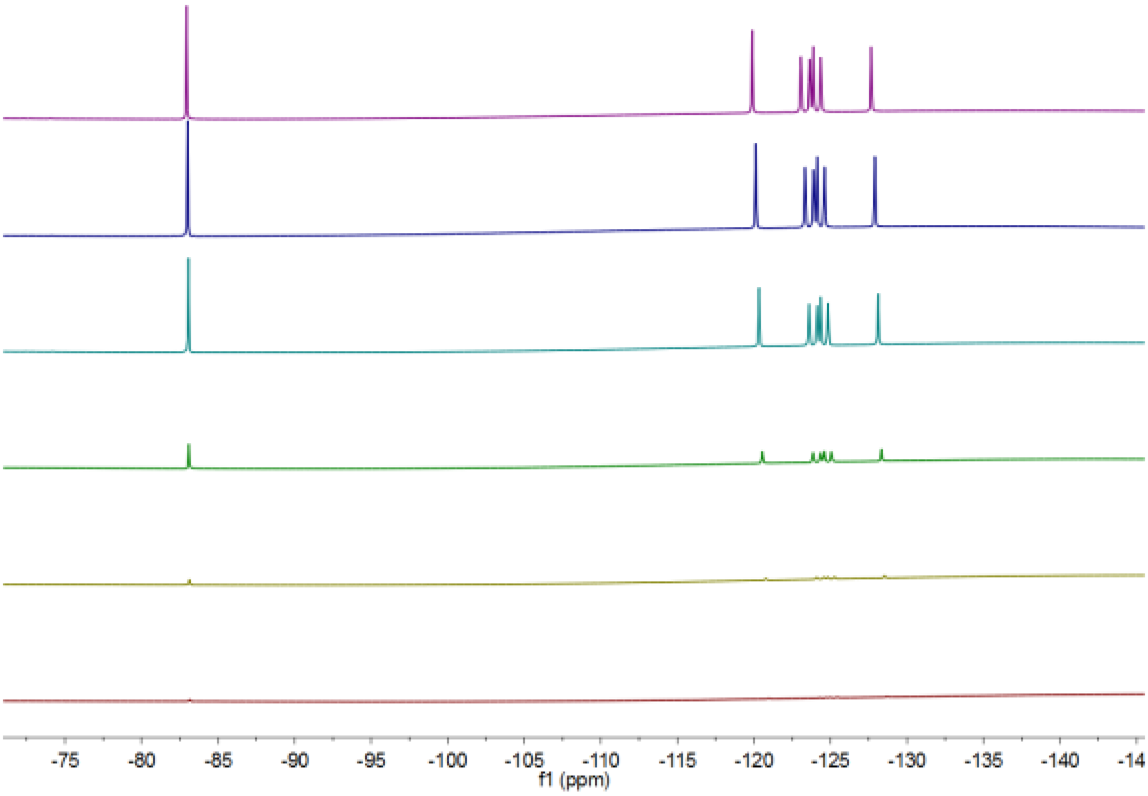

Figure S20. VT ^{19}F NMR (470 MHz) free ligand **3**, 2% DMSO-d_6-D_2O. The spectra were collected from 25 °C (bottom) to 120 °C (top) with 15 or 20 °C increments.

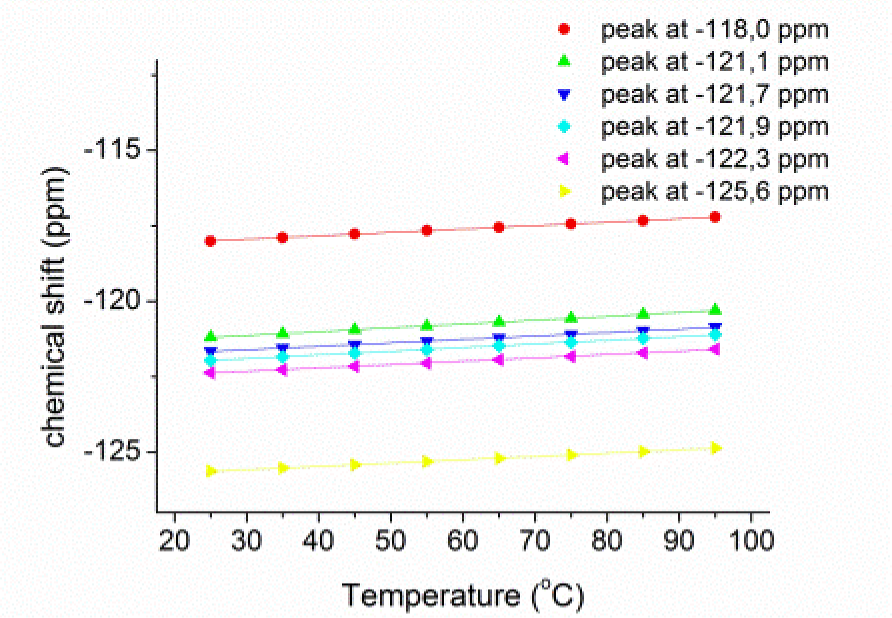

Figure S21. VT ^{19}F NMR chemical shift vs temperature for **3-Fe** 2% DMSO-d_6-D_2O.

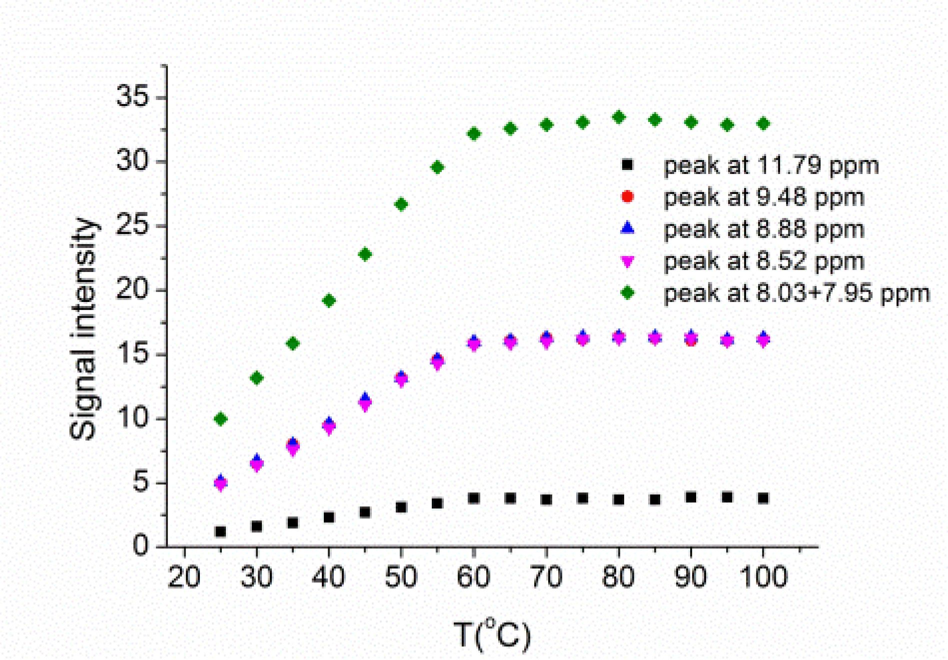

Figure S22. Variation of ^{1}H NMR signal intensity with temperature for **3-F**e-gel 2% DMSO-d_6-D_2O.

$$ln(Sol) = -\frac{3713}{T_{eq}} + 7.03$$

Equation S1. Van't Hoff equation obtained from VT ^{1}H NMR.

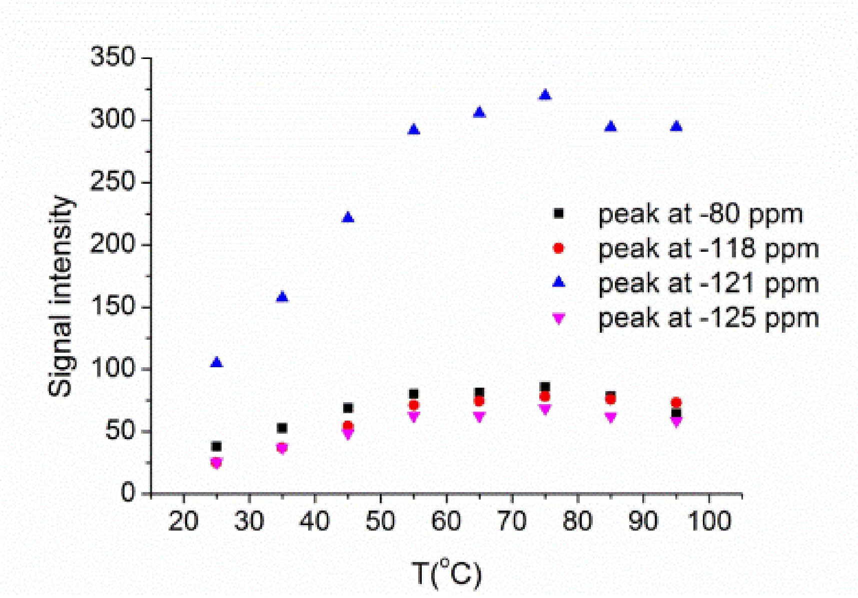

Figure S23. Variation of ^{19}F NMR signal intensity with temperature for **3-Fe**-gel 2% DMSO-d_6-D_2O.

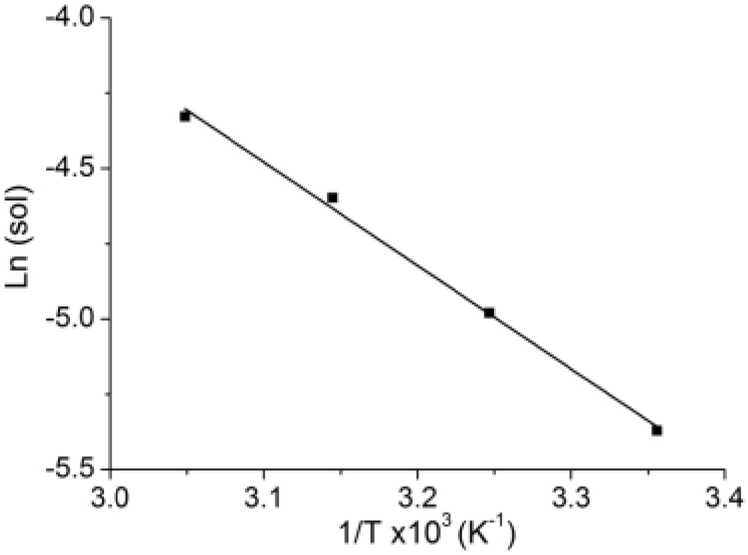

Figure S24. ln (Sol) against the reciprocal of the temperature by ^{19}F NMR.

$$\boldsymbol{ln(Sol) = -\frac{3437}{T_{\mathrm{eq}}} + 6.17}$$

Equation S2. Van’t Hoff equation obtained from VT ^{19}F NMR.

ATR-FTIR

The attenuated total reflectance Fourier transform infrared (ATR-FTIR) spectrum was measured with a Shimadzu IRAffinity-1 spectrometer. The transmittance spectrum was collected using a spectral resolution of $\Delta\nu = 1\ \mathrm{cm}^{-1}$, accumulating 32 scans and performing the ATRcorrection (penetration depth mode).

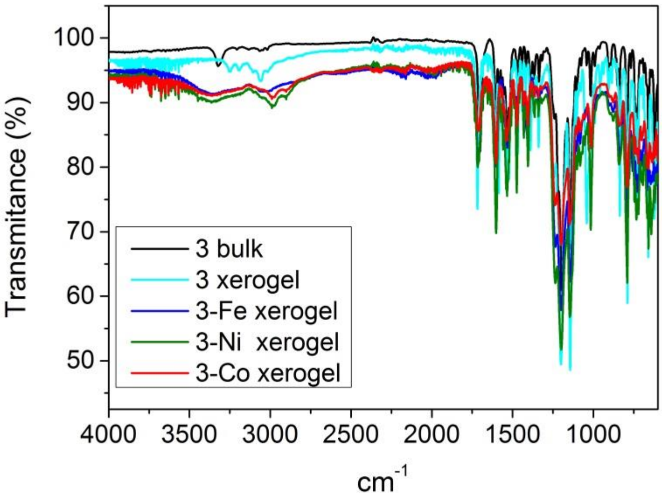

Figure S25. IR spectra of ligand **3** as bulk and xerogel of **3**, **3-Fe, 3-Co** and **3-Ni**.

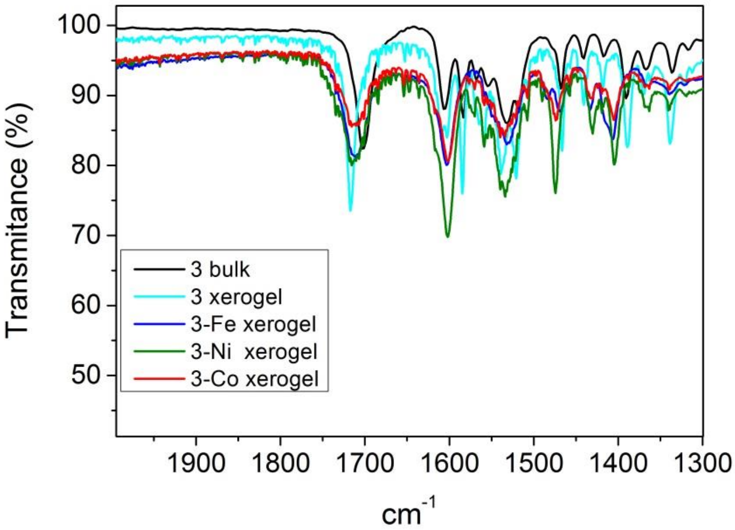

Figure S26. IR spectra of ligand **3** as bulk and xerogel of **3**, **3-Fe, 3-Co** and **3-Ni**.

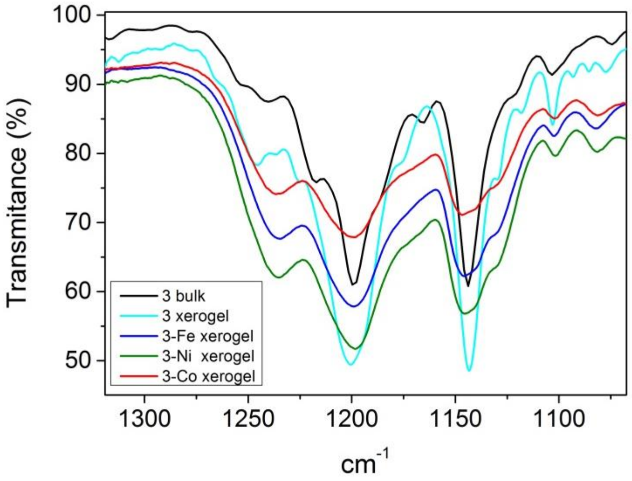

Figure S27. IR spectra of ligand **3** as bulk and xerogel of **3**, **3-Fe, 3-Co** and **3-Ni**.

References

1. *CrysAlisPro 2015, Rigaku Oxford Diffraction. Version 1.171.38.43*.
2. G. Sheldrick, *Acta Crystallographica Section A*, 2008, **64**, 112-122.
3. O. V. Dolomanov, L. J. Bourhis, R. J. Gildea, J. A. K. Howard and H. Puschmann, *Journal of Applied Crystallography*, 2009, **42**, 339-341.
4. G. Sheldrick, *Acta Crystallographica Section A*, 2015, **71**, 3-8.